

Report UWAL-JN-2001-01

Final Report

Cooperative Agreement NCC 2-5315

Automatic Fringe Detection for Oil Film
Interferometry Measurement of Skin Friction

Jonathan W. Naughton, Principal Investigator

Robert K. Decker

Department of Mechanical Engineering

Farhad Jafari

Department of Mathematics

University of Wyoming

Laramie, Wyoming 82071

November 26, 2001



Abstract

This report summarizes two years of work on investigating algorithms for automatically detecting fringe patterns in images acquired using oil-drop interferometry for the determination of skin friction. Several different analysis methods were tested, and a combination of a windowed Fourier transform followed by a correlation was found to be most effective. The implementation of this method is discussed and details of the process are described. The results indicate that this method shows promise for automating the fringe detection process, but further testing is required.



1 Introduction

The measurement of skin friction has been a challenge for the aerodynamic measurement community. Problems with accuracy, spatial resolution, and application in flows with pressure gradients, separation, and re-attachment have confronted engineers attempting skin friction measurements. Fortunately, a technique has been developed over the past 25 years that eliminates most of the problems described above. This technique, oil film interferometry, has a rigorous physical basis, requires no calibration, and has been applied in complex, three-dimensional flows.

Although there have been several implementations of oil-film interferometry for skin friction measurement [Monson et al., 1993, Naughton and Brown, 1996, Garrison and Ackman, 1998], one of the most popular techniques involves the use of oil drops [Tanner and Kulkarni, 1976, Zilliac, 1996]. In this technique, many small drops of oil are applied to a model. As an aerodynamic flow develops on the model, the oil flows back in the direction of surface streamlines. At any location in the thin film that develops, the oil height decreases at a rate proportional to the shear stress acting on it. Thus, by determining the height of the oil film, the shear stress may be calculated.

To determine the height of these very thin oil films, Tanner and Blows [1976] suggested the use of interferometry. When an oil-film is illuminated using monochromatic light, light reflects from both the oil-air and oil-surface interfaces. When these two beams are recombined, the degree of constructive or destructive interference they experience is controlled by the path length difference. This path length difference is dependent on the oil-film thickness, and thus the oil-film height can be determined from the amount of constructive or destructive interference observed. The data for these experiments are images of the interference pattern (interferograms).

In oil-drop interferometry, many of these interference patterns can occur in a single image. Fig. 1 shows a transport wing with hundreds of interference fringe patterns. Using oil-drop interferometry, a single shear stress value is determined from each of these interference patterns. Obviously, a strong point of this technique is that many surface shear stress vectors can be obtained during a single test.

Currently images such as that in Fig. 1 are analyzed with software that requires interactive selection of the fringe patterns [Zilliac, 1999]. Although this process works well, it can be tedious if hundreds of interference fringes in an image need to be selected. In a typical test, ten to a hundred images

may be required to cover a range of operating conditions, and the time required for analyzing these images, most of which is devoted to selecting fringe patterns, becomes prohibitive. If a means of automating the fringe selection process could be developed, the tedious nature of this process would decrease significantly.

2 Problem Statement

The issue that was considered during the course of this study was the development of a quick, robust method for automatically identifying fringe patterns in interferograms acquired using oil-film interferometry. The method was required to handle the noise typically present in these images and was targeted to identify 75% of the fringes present in a given image (i.e. 75% of those that could be picked out with the eye). It was also desired that this method could be easily implemented into existing software.

3 Objectives

1. Identify a fringe detection scheme that successfully identifies fringe patterns in interferograms obtained using thin-oil-film interferometry for shear stress measurement.
2. Develop a library of image analysis routines written in C used for fringe identification.
3. Test the fringe detection schemes in various oil-film interferograms.
4. Document the limitations of the technique.

4 Results

This study has identified a promising method for the automatic detection of fringes in an oil-film interferogram. The method has been implemented in `c`-code, but it has yet to be rigorously tested. Work on this aspect will continue after the funding under the current grant has expired. Our ongoing use of oil-film interferometry for skin friction measurements will provide ample opportunities to test and to improve the methodology described here.



Figure 1: Image of a transport wing with many interference patterns generated by oil drops applied to the model.



This section of the report will be broken into the following sections. First, a brief description of the analysis techniques that were identified for fringe identification will be discussed. Second, a summary of the analysis routines (not included in the report) developed as part of this work will be described. Finally, the limitations of the current approach will be discussed.

4.1 Fringe Detection Method

Several image analysis approaches have been investigated in an attempt to identify the most effective fringe identification method. Windowed Fourier transforms, correlation methods, wavelets, and convolutions methods have all been investigated. Details of the different approaches are described in depth by [Decker et al., 2000, Decker and Naughton, 2001] and will not be repeated here. The most effective method is a combination of the windowed Fourier transform and the correlation method. This combination provides a computationally inexpensive way to combine a technique that is perfectly localized in frequency (to identify the fringe characteristic frequency) with a technique that is localized in space (so the fringes location is known). The power of this technique compared to wavelet methods (which can simultaneously identify location and frequency) is that any second function can be used for the correlation and is not limited to the few wavelet functions available. Since the interference patterns are well represented by sine and cosine waves, these functions are the appropriate “interrogation” functions.

The implementation of the combined WFT/correlation approach is described using a one-dimensional example. First, a window with a dimension that is a fraction of the total image size is selected and is represented by the red lines in Fig. 2 (a). A larger representation of the windowed portion of the original intensity signal is shown in Fig. 2 (b). The Fourier transform $I(f_x)$ of the intensity i in this windowed region is obtained using:

$$I(f_x) = \mathcal{F}(i), \quad (1)$$

where f_x is the spatial frequency and $\mathcal{F}(i)$ represents the Fourier transform of i . The auto-spectral density of the intensity signal in Fig. 2 (b)

$$S_{i,i} = \frac{1}{n\Delta x} |I(f_x)|^2 \quad (2)$$

is shown in Fig. 2 (c). The frequency f_x at which $S_{i,i}$ has the largest magnitude is determined. Note that, in Fig. 2 (b), the dominant frequency is the

fifth non-zero frequency. If the magnitude of the dominant frequency is sufficiently large, a one-cycle cosine wave with a frequency equal to that of the dominant frequency is generated. This “interrogation fringe” i_{if} , shown in Fig. 2 (e), is then correlated with the appropriately padded, zero-mean windowed signal (see Fig. 2 (d)) using the following process. First, the Fourier transform $I_{if}(f_x)$ of the interrogation fringe is determined as described in Eq. 1. The auto-spectral density function $S_{if,if}$ is determined as described in Eq. 2 and the cross-spectral density function is determined using

$$S_{i,if} = \frac{1}{N\Delta x} S_{i,i} S_{if,if}^* \quad (3)$$

The cross-correlation $R_{i,if}$ is then calculated by taking the inverse FFT

$$R_{i,if} = \mathcal{F}^{-1}(S_{i,if}), \quad (4)$$

where \mathcal{F}^{-1} represents the inverse Fourier transform. In a similar manner, the auto-correlations $R_{i,i}$ and $R_{if,if}$ are determined. Finally, the cross correlation coefficient $\rho_{i,if}$ is calculated using

$$\rho_{i,if} = \frac{R_{i,if}}{\sqrt{R_{i,i}(0)R_{if,if}(0)}}, \quad (5)$$

where $R_{i,i}(0)$ and $R_{if,if}(0)$ represent the value of the auto-correlations at an offset of 0. The results of the correlation process are shown in Fig. 2 (e). When the correlation coefficient approaches 1 or -1, there is a strong correlation between the interrogation fringe and the original intensity. Thus, high values of the $\rho_{i,if}$ correspond to valleys in the original image and the lowest values of $\rho_{i,if}$ correspond to the peaks. Figs. 2 (a), (c) and (e) contain numbered peaks and valleys that show the relationship between the peaks and valleys in $\rho_{i,if}$ and the peaks and valleys in the original signal.

If this same approach is applied to a region that contain no fringes, a different result is evident. Fig. 3(a) shows the analysis of a region of the image containing no fringes. The auto-spectrum of the highlighted portion of the image seen in Fig. 3(c) does have significant energy in the first non-zero frequency, but this is probably due to the decreasing intensity observed in Fig. 3(b). In this case, a criterion that the energy fall in a higher frequency eliminated this from further consideration.

With some effort, the combined WFT/correlation approach can be extended to two-dimensional images. As in the one-dimensional case, a windowed Fourier transform is applied to a windowed region of the original



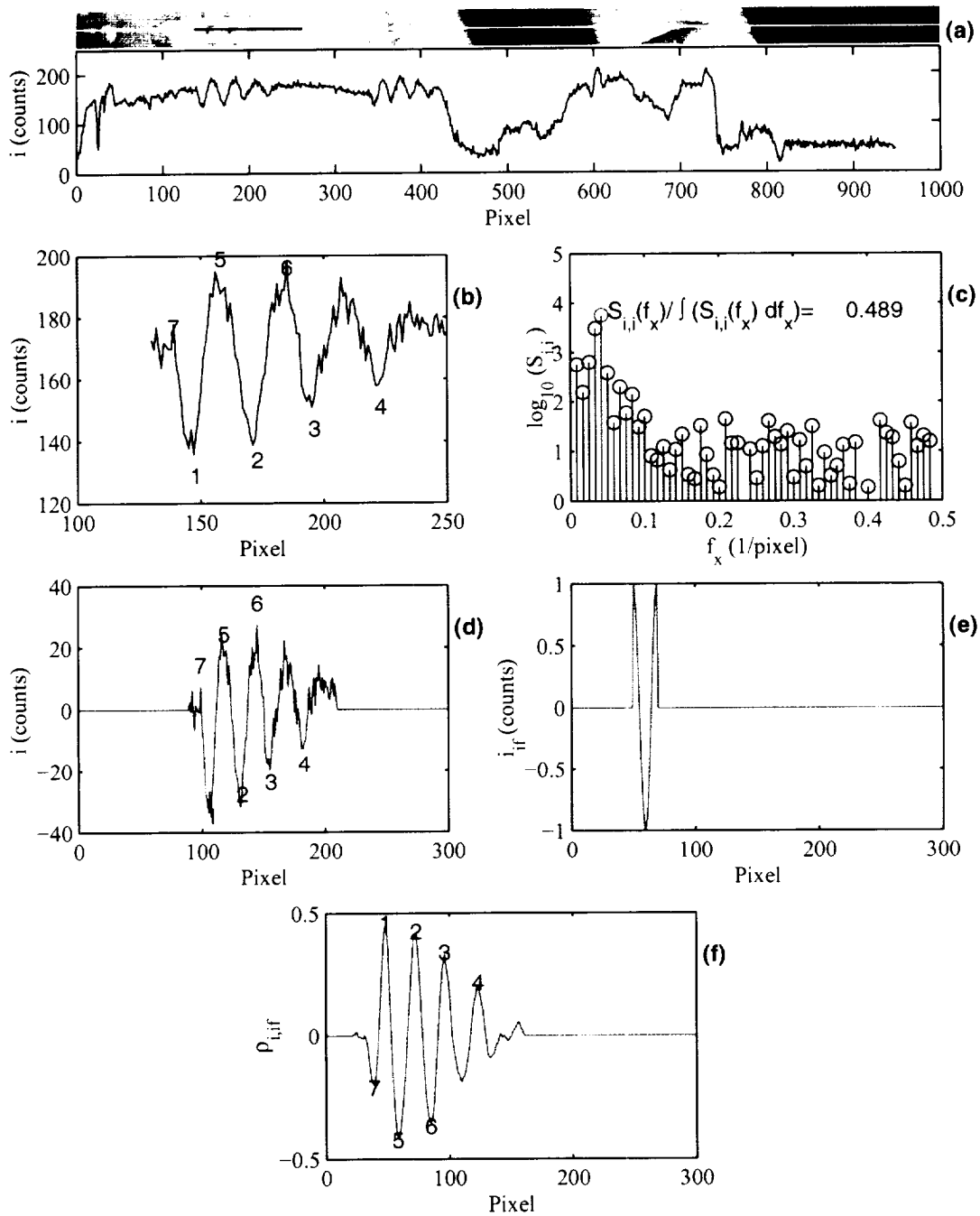


Figure 2: One dimensional windowed Fourier transform (WFT) and correlation method: (a) portion of original image and plot of intensity along a line; (b) windowed portion of original intensity record in (a); (c) auto-spectral density of the data in (b); (d) padded windowed data; (e) interrogation fringe; (f) cross-correlation coefficient of (d) and (e).

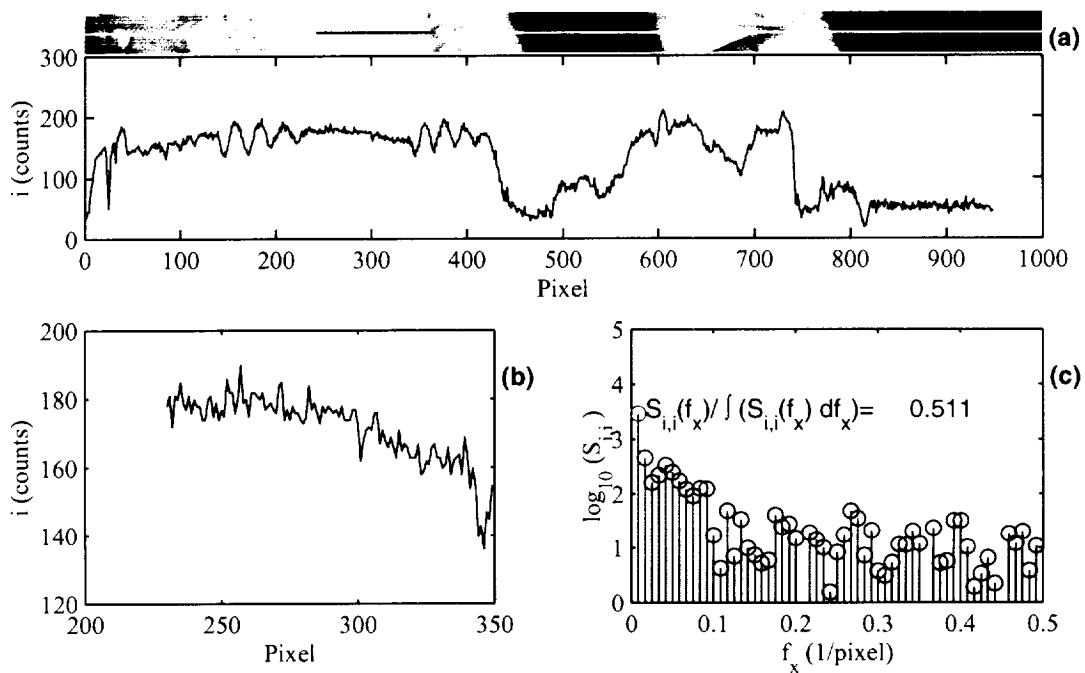


Figure 3: One dimensional windowed Fourier transform (WFT) and correlation method for a region of an image containing no fringe: (a) portion of original image and plot of intensity along a line; (b) windowed portion of original intensity record in (a); (c) auto-spectral density of the data in (b).

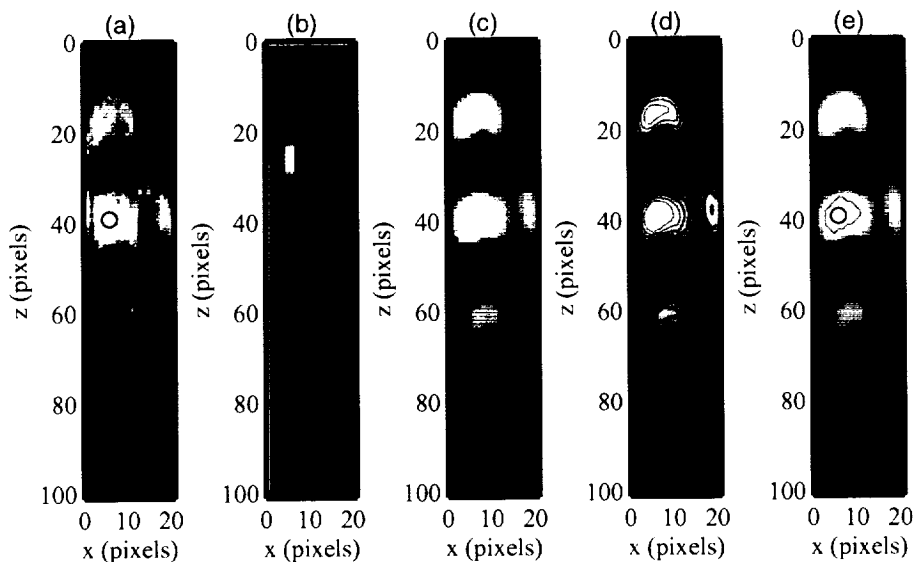


Figure 4: Two dimensional windowed Fourier transform (WFT) and correlation method: (a) portion of original image with peak and valleys detected indicated; (b) interrogation fringe; (c) cross-correlation coefficient of (a) and (b); (d) cross-correlation coefficient overlaid with contours of the cross-correlation coefficient; and (e) cross-correlation coefficient overlaid with contour used for eliminating high correlation coefficient values in the neighborhood of a peak or valley and symbols indicating the location of the peaks and valleys.

images (Fig. 4 (a)). The Fourier transform of this figure now contains frequency information in both the horizontal x and vertical z directions. This frequency information is used to determine the “interrogation fringe” that is shown in Fig. 4 (b). Cross-correlating this interrogation fringe with the original image yields the cross-correlation coefficient $\rho_{i,if}$ shown in Fig. 4 (c) as a gray-scale image. As is evident in the cross-correlation coefficient, the peaks and valleys of the original interferogram are the maxima and minima of the correlation coefficient. It is also evident that this process acts as a filter in that the interference fringes remain and much of the extraneous information (most of it not desired) from the original image is eliminated. Fig. 4 (d) shows $\rho_{i,if}$ contours on top of the gray-scale representation of $\rho_{i,if}$ and indicates that $\rho_{i,if}$ is a smooth function near the peaks and valleys of the interferogram.



To isolate the peaks and valleys of the fringes from the correlation coefficient $\rho_{i,if}$, the following approach is used. First, the array of correlation coefficients is sorted from maximum to minimum values. The maximum correlation coefficient is compared against a threshold, and, if it exceeds the threshold, it is designated as an interference peak. To ensure that no other values associated with this peak are identified as peaks themselves, a region surrounding the fringe is isolated. This is accomplished by determining a contour around the peak at a level substantially below the peak value. All of the values within this region are set to zero, so they will not be identified as separate peaks. The most negative correlation coefficient is next considered in the same way. Alternating between the highest and lowest correlation coefficients, this process is repeated until there are no longer maxima/minima that exceed the prescribed threshold.

The results of applying this process to the original windowed data in Fig. 4 (a) are shown in Fig. 4 (e). In this figure, the $\rho_{i,if}$ values (plotted as a gray-scale image) are overlaid with the contour used to isolate the peaks and valleys. The symbol in the center of the contour identifies the peak or valley. In this image, it is evident that one peak and one valley have been found. Symbols locating the peaks and valleys of the fringe are also overlaid on the original image in Fig. 4 (a).

The image processing routines that perform these functions have been implemented in c-code. The next section briefly summarizes the purpose of each routine.

4.2 Library of Image Analysis Routines

To implement the fringe detection algorithms described above, several C-programs were acquired and several were written. Below is a brief description of each of C-program and table 1 provides a summary of the most important programs.

Fast Fourier Transform

This file implements the multivariate complex Fourier transform, computed in place using mixed-radix Fast Fourier Transform algorithm. The original FORTRAN code was written by R.C. Singleton of the Stanford Research Institute in September 1968. The code was translated to C at a later date.

Table 1: Description of various C routines used for fringe detection.

Routine	Description
fftn.c	Performs the Fast Fourier Transform (FFT)
corrcoef.c	Determines the correlation coefficient
rfringe.c	Creates an interrogation fringe
fdutils.c	Fringe detection utilities
fftutils.c	FFT utilities
index.c	Determines indices of array values from low to high
scont.c	Finds a discrete contour
mask.c	Creates a mask within a closed contour
bitmap.c	Reads and writes 8-bit gray-scale images

Interrogation Fringe Creation

This subroutine generates an interrogation fringe based on the dominant frequency returned from FFTN.

Correlation Coefficient

This subroutine calculates the cross-correlation coefficients of two input arrays.

Fringe Detection and FFT Utilities

These files contain several utility routines used for manipulation of FFT data and other processes associated with fringe detection.

Index an Array

This subroutine creates an array of indices of an array ordered from lowest value to highest value. This routine is used as part of the correlation peak and valley detection.

Discrete Contour Routine

This subroutine determines a closed contour in an image. It does this without interpolation by simply finding the locations of the pixel that most closely



approximate the desired contour level. This routine is used as part of the correlation peak and valley detection.

Mask an Enclosed Area

This subroutine creates a mask for an image that fills the interior of an enclosed area with zero and sets all other values to one. This routine is used as part of the correlation peak and valley detection.

Read a Bitmap Image

This file contains subroutines for creating, reading, and writing bitmap images.

Sample Fringe Detection Program

A program that integrates the programs listed above into a single routine is provided. A brief description of the logic of this program is provided here. First, an image is read into memory from a bitmap file (Windows bitmap for this demonstration). A windowed region of this image is extracted and FFTN is used to determine the Fourier transform. The most dominant frequency of the Fourier transform is determined, and, if the energy contained in that frequency is large enough and the frequency falls within a user-chosen interval, the window is processed further to determine the location of the fringe pattern within the image. If the peak frequency does not meet these criteria, the program extracts the next windowed region and continues.

If a peak frequency meets the user-specified criteria, an interrogation fringe is created with CRTIFRNG using the x and z frequencies associated with the peak frequency. First, an image twice the size of the original image is created and filled with a single frequency cosine corresponding to the dominant frequency in the windowed Fourier transform. A mask is then created that leaves a single-cycle cosine fringe at the center of the image. Finally, this fringe is translated to the upper left-hand corner of the image for further processing.

In addition to the interrogation fringe, the original image is also prepared for further processing. First, the DC component of the Fourier transform array is zeroed and then is inverse transformed to create a zero-mean image. This image is then padded to produce an image twice the size of the

original image. The zero-mean image is located in the center of this new array.

Next, the cross-correlation coefficient of the padded source image and the interrogation fringe is determined using CORRCOEFF. These cross-correlation coefficients provide the information necessary to locate the fringe peaks and valleys.

The peaks and valleys of the interferogram are isolated using a three step process. First an array of indices of the cross-correlation coefficient array sorted from low to high values is created using INDEX. This index array is then analyzed from the highest value down and the lowest value up. Once a candidate peak has been located it is accepted or rejected by comparing its correlation-coefficient value to a user-specified threshold. If a peak value falls below the accepted threshold, it is rejected and no further peaks will be found that pass the criteria. If a peak value does exceed the user-specified threshold, it is recorded as a peak. To eliminate other neighboring points of the peak from being identified as peaks themselves, SCONT is used to determine a closed contour of a specified level around the peak. A mask is then created using MASK that zeros all values of the correlation coefficient within the closed contour. The next highest value in the index array is then determined and the process is repeated. A similar approach is used for to isolate the valleys.

The process outlined above is repeated for various windowed regions in the original image thus enabling the analysis of the entire image. The coordinates of each peak and valley found are written to a file.

4.3 Limitations

A complete list of the limitations of the fringe identification method discussed here has not been fully developed at this time. Further testing of the method on a wide variety of image is required before all the limitations are known. However, the known limitations are briefly discussed below.

First, the eye is still more effective at determining fringe patterns than is the fringe detection method. Peaks and valleys in the interferogram that are apparent to the eye are missed by the technique. The reason for this is that, in order to have a lower limit on correlation coefficient to avoid detecting "false" peaks and valleys, some of the peaks and valleys with low visibility will be missed. The position taken here is that it is better to miss identifying some low-visibility peaks and valleys in order to prevent the detection of

erroneous peaks and valleys.

Another known limitation is that, on occasion, a feature will fool the fringe identification process into thinking that it has found a fringe peak or valley. Fortunately, the false peak or valley identified is normally isolated, and a rejection criteria could be developed based on a proximity of a peak to a valley or vice versa.

Another limitation that is associated with finding false peaks/valleys is that some good fringes that should be detected are missed because the dominant frequency in the FFT is associated with a false peak or valley and the good peaks and valleys are rejected since their power is lower. The missed fringes can often be recaptured by using window overlapping that often eliminates the spurious fringe from a subsequent window in which the missed fringe appears. Also, slightly changing the frequency rejection criteria will often eliminate the spurious fringe.

5 Publications and Patents

A list of publications that are a direct result of this work are listed below:

R. K. Decker and J. W. Naughton. Automated interference fringe pattern recognition. Submitted for publication in *Journal of the Optical Society of America A*.

R. K. Decker and J. W. Naughton. Improved fringe imaging skin friction analysis using automated fringe identification. AIAA Paper 2001-0557, January 2001.

R.K. Decker, J.W. Naughton, and F. Jafari. Automatic fringe detection for oil film interferometric skin-friction measurement. In I. Grant and G.M. Carlomagno, editors, *Proceedings of the 9th International Symposium on Flow Visualization, 2000*. (on CD ROM, ISBN 0 9533991 1 7).

No patents have been obtained or filed for under this grant.

6 Student Involvement

This grant supported, in part, Robert Decker through part of his undergraduate studies and throughout his graduate work. The work reported here is

included in Robert's Masters thesis that will be completed in December 2001.

References

- R. K. Decker and J. W. Naughton. Improved fringe imaging skin friction analysis using automated fringe identification. AIAA Paper 2001-0557, January 2001.
- R.K. Decker, J.W. Naughton, and F. Jafari. Automatic fringe detection for oil film interferometric skin-friction measurement. In I. Grant and G.M. Carlomagno, editors, *Proceedings of the 9th International Symposium on Flow Visualization*, 2000. (on CD ROM, ISBN 0 9533991 1 7).
- T.J. Garrison and M. Ackman. Development of a global interferometer skin-friction meter. *AIAA Journal*, 36(1):62-86, 1998.
- D.J. Monson, G.G. Mateer, and F.R. Menter. Boundary-layer transition and global skin friction measurement with an oil-fringe imaging technique. SAE Paper No. 932550, September 1993.
- J.W. Naughton and J.L. Brown. Surface interferometric skin-friction measurement technique. AIAA Paper 96-2183, June 1996.
- L.H. Tanner and L.G. Blows. A study of the motion of oil films on surfaces in air flow, with application to the measurement of skin friction. *Journal of Physics E: Scientific Instrumentation*, 9(3):194-202, March 1976.
- L.H. Tanner and V.G. Kulkarni. The viscosity balance method of skin friction measurement: Further developments including applications to three-dimensional flow. *Journal of Physics E: Scientific Instrumentation*, 9: 1114-1121, December 1976.
- G. Zilliac. Further developments of the fringe-imaging skin friction technique. NASA-TM 110425, NASA-Ames Research Center, December 1996.
- G. G. Zilliac. The fringe-imaging skin friction technique pc application user's manual. NASA-TM 1999-208794, NASA-Ames Research Center, 1999.

